Atmospheric Environment xxx (2009) 1–10

Contents lists available at ScienceDirect

Atmospheric Environment

journal homepage: www.elsevier.com/locate/atmosenv

Inferring episodic atmospheric iron fluxes in the Western South Atlantic

Heitor Evangelista [a,*], Juan Maldonado [a,b], Elaine A. dos Santos [a], Ricardo H.M. Godoi [c], Carlos A.E. Garcia [d], Virginia M.T. Garcia [d], Erling Jonhson [e], Kenya Dias da Cunha [f,g], Carlos Barros Leite [f], René Van Grieken [h], Katleen Van Meel [h], Yaroslava Makarovska [h], Diego M. Gaiero [i]

[a] Universidade do Estado do Rio de Janeiro/LARAMG. Pav. HLC. Subsolo, Rua São Francisco Xavier, 524. Maracanã, Rio de Janeiro – RJ 20550-013, Brazil
[b] Universidade Federal Fluminense/Departamento de Geoquímica Ambiental, Outeiro São João Batista, s/n° – Centro – Niterói, RJ 24020-150, Brazil
[c] Environmental Engineering Department, Federal University of Paraná/UFPR, P.O. Box 19011, 81531-990 Curitiba, PR, Brazil
[d] Universidade Federal do Rio Grande/Laboratório de Oceanografia Física, Av. Itália km 8, Rio Grande, RS 96201-900, Brazil
[e] Universidad Magallañes/Instituto de Física, Cassila 113-D, Punta Arenas, Chile
[f] PUC-RIO, Laboratório van de Graaff, Rua Marques de São Vicente, 225, Rio de Janeiro – RJ 22451-041, Brazil
[g] IRD/CNEN. Av, Slavador Allende s/n, Rio de Janeiro – RJ 22780-160, Brazil
[h] University of Antwerp/Department of Chemistry/Micro and Trace Analysis Centre, 2610 Antwerp, Belgium
[i] CIGeS, FCEFyN, Universidad Nacional de Cordoba, Avda. Velez Sarsfield 1611, X50166CA Cordoba, Argentina

ARTICLE INFO

Article history:
Received 20 January 2009
Received in revised form
2 November 2009
Accepted 6 November 2009

Keywords:
Patagonia
Iron deposition
Western South Atlantic
Aerosols

ABSTRACT

Iron (Fe) and other trace elements such as Zn, Mn, Ni and Cu are known as key-factors in marine biogeochemical cycles. It is believed that ocean primary productivity blooms in iron deficient regions can be triggered by iron in aeolian dust. Up to now, scarce aerosol elemental composition, based on measurements over sea at the Western South Atlantic (WSA), exist. An association between the Patagonian semi-desert dust/Fe and chlorophyll-a variability at the Argentinean continental shelf is essentially inferred from models. We present here experimental data of Fe enriched aerosols over the WSA between latitudes 22°S–62°S, during 4 oceanographic campaigns between 2002 and 2005. These data allowed inferring the atmospheric Fe flux onto different latitudinal bands which varied from 30.4 to 1688 nmolFe m^{-2} day^{-1} (October 29th–November 15th, 2003); 5.83–1586 nmolFe m^{-2} day^{-1} (February 15th–March 6th, 2004) and 4.73–586 nmolFe m^{-2} day^{-1}(October 21st–November 5th, 2005).

1. Introduction

It has been proposed that the micronutrient Fe plays a key role as limiting factor for phytoplankton growth rate and structuring plankton communities in the world oceans (Moore et al., 2002). A deficiency of Fe in seawater may prevent the complete biological assimilation of available nitrate and influences plankton species composition in open-ocean environments. The "Fe hypothesis" was postulated by John Martin in 1991 who stated that phytoplankton may not grow at optimal rates in some ocean areas, characterized as high nutrient low chlorophyll (HNLC) (Bucciarelli et al., 2001). At those sites the major phytoplankton limiting factor is attributed to dissolved Fe in the euphotic zone. An important parameter in the delivery of terrigenous material (including Fe) from land to the sea is the surface winds and it is believed to be the dominant factor at most remote ocean sites (Duce and Tindale, 1991; Sarthou et al., 2003). An evidence of this process is the occurrence of mineral types as kaolinite and illite in sea bottom sediments off the coast, where no or very few fluvial sources could be associated to (Prospero, 1981). Although some studies have inferred the Fe atmospheric deposition flux into the Western South Atlantic (WSA), based on models and considerations of dust emission from the Patagonian semi-desert (e.g.: Erickson et al., 2003), so far no reproducible experiments have been conducted to measure the in situ Fe flux in the ocean to validate the estimates. In this work we analyze data obtained from four oceanographic cruises concerning the Fe concentrations and fluxes, associations with terrigenous elements, potential anthropogenic sources and the atmospheric transport between South America and WSA continental shelf.

2. Study area

Oceanographic campaigns were basically developed over the continental shelf within the latitudinal band 22–62°S. The

* Corresponding author. Tel./fax: +55 21 2334 0133.
E-mail addresses: evangelista.uerj@gmail.com (H. Evangelista), juantsi@yahoo.com.br (J. Maldonado), rhmgodoi@hotmail.com (R.H.M. Godoi), dfsgar@furg.br (C.A.E. Garcia), docvmtg@furg.br (V.M.T. Garcia), ejohn@ona.fi.umag.cl (E. Jonhson), kenya@ird.gov.br (K. Dias da Cunha), cvbl@vdg.fis.puc-rio.br (C.B. Leite), rene.vangrieken@ua.ac.be (R. Van Grieken), dgaiero@com.uncor.edu (D.M. Gaiero).

1352-2310/$ – see front matter © 2009 Elsevier Ltd. All rights reserved.
doi:10.1016/j.atmosenv.2009.11.018

continental land associated to that encloses part of Southeast Brazil, South of Brazil, the coast of Uruguay and Argentine, up to the South Shetland Islands, at Northern Antarctic Peninsula. One of the major continental influencing region of this study is the Patagonian semi-desert. Its climatology is controlled by the persistent westerly winds that blow from the Pacific Ocean, though the Andean Cordillera where they discharge most of their water content, and continuing as dry winds to the East (Iriondo, 2000). The annual precipitation at the semi-desert domain is less than 200 mm and it is concentrated in the fall-winter seasons. The partial lack of soil moisture, sparse vegetation cover and strong surface winds provide the appropriate conditions for dust emission (Gaiero et al., 2003). In general, dust activity (resuspension) is higher during the summer, although winter and fall events have also been reported (Gassó and Stein, 2007). Aerosol samples were collected on board the Oceanographic vessel "Ary Rongel" of the Brazilian Navy. Data were obtained underway from the City of Rio de Janeiro/Brazil to King George Island in the South Shetland Islands.

3. Methods

Total Fe flux was obtained from both in situ aerosol measurements over sea and modeled data that estimated deposition velocities and wet precipitation at the study region. The dry component of the Fe flux was estimated by a simple model based on the Fe concentrations determined at the fine and coarse aerodynamic modes, sampled during the oceanographic cruise of 2003, 2004 and 2005, multiplied by the corresponding deposition velocities of 0.001 m s^{-1} and 0.02 m s^{-1}, according to Duce et al., 1991. Especially for the 2002 campaign, the Fe Mass Median Aerodynamic Diameter (MMAD) was calculated using a six-stage cascade impactor. In this case, the deposition velocities for each aerosol diameter was estimated by a model proposed by Slinn and Slinn (1980), which considers the marine environment characteristics and measured in situ wind velocity. Since in the geographic context of this work, precipitation is expected to occur, the wet component of Fe flux was estimated using daily precipitation rate maps averaged for one month (November for the year 2003, February for 2004 and October for 2005). Precipitation data (enclosing: 40–70°W and 22–60°S) were provided by the NOAA/ESRL, at the website http://www.cdc.noaa.gov/, and superimposed to the ship tracks in a geo-referenced system (ARC VIEW).

3.1. On board aerosol sampling

Atmospheric samplings occurred during the following oceanographic campaigns: one in the period October–November of 2002, that covered the latitudinal band 22–52°S, specially conducted to integrate aerosols into six aerodynamic diameters; followed by 3 main campaigns: the first between October 29th and November 15th, 2003; the second between February 15th and March 6th, 2004; and the third between October 21st and November 5th, 2005. Mean distances between the ship tracks and coast line varied from 300 to 900 km. During all campaigns, the samplings were performed using a wind sector control system to prevent from the ship's exhaust contamination. The aerosol inlet (a cylindrical tube of 20 cm length and 15 cm width) was used to prevent the filters from sea spray. It was positioned at the top of the ship (10 m a.s.l.), 50 m away from the ship stack's emission, while the pumping unit was installed inside the ship and consisted of: (1) one high volume pump (one-head GAST model); (2) an air flow monitor; and (3) a wind sector sampling control that is an electronic device connected to an anemometer (installed besides the inlet compartment), a datalloger, a two-way electrical valve and the pumps. The system was programmed to interrupt the aerosol sampling any time the wind direction is inside an angular sector (named "dirty sector") of 60° centered at a line between the inlet and the ship's exhaust. Therefore, if the wind turns to the "dirty sector" the air flow connection between the filter holder and the pump unit is interrupted through a two-way electrical valve. In parallel we used an aethalometer (Magee Scientific, model Ae-10) to monitor the aerosol black carbon (BC) in 30 min-resolution. Both aerosols and BC inlets were positioned together. BC data allowed investigating the effectiveness of the aerosol discrimination system. Data of BC of these campaigns were discussed in Evangelista et al. (2007). Particularly during the 2002 campaign we used a six-stage cascade impactor, with operational flow rate of 12.5 ± 0.6 L min^{-1} and cutoff diameters of 19.9, 9.9, 4.7, 2.4, 1 and 0.64 μm. Fe concentrations were analyzed by PIXE technique, Dias da Cunha et al. (1998). For 2003 and 2004 campaigns, a "May cascade impactor" (May, 1975), was used to collect particles in two aerosol size ranges: 0.5–2 μm and 2–8 μm. In this system, airborne particles are forced to collide, by inertial impactation, over a glass plate coved with a thin silver film. Detected particles were individually analyzed by EPMA (Electron Probe Micro-Analysis) to determine the elemental mass concentration. Additionally, a stacked filter unit composed by a two-stage filter holder, to collect aerosols in fine and coarse modes (Nuclepore, 1987) was used. Aerosols were deposited onto sequential Nuclepore polycarbonate membrane filters of 47 mm of diameter. Each holder was composed by an upper filter with membrane pore size of 8 μm and a bottom filter of 0.4 μm. In this system the collection efficiency is a function of the aerosol aerodynamic diameter, and the cutoff diameter is defined at a 50% efficiency collection (Parker et al., 1977). Considering our air flow range of 12–17 sLpm (standard Liter per minute), the cutoff diameter for the coarse mode is ~2 μm (John et al., 1983). For the above air flow, the inlet characteristic provides an aerosol cutoff diameter of ~10 μm (Cahill et al., 1979). This allowed the selection of particles with diameters (d_p) < 2 μm and 2 < d_p < 10 μm for the fine and coarse modes, respectively. The use of this technique is particularly valid for samplings of short duration conducted at remote regions, where atmospheric aerosol collection is typically very low. Filters containing particles were submitted to EDXRF technique. A summary of the aerosol techniques and oceanographic cruises is presented in Table 1. Calibration and inter-comparisons of PIXE and EDXRF are described in Calzolaia et al. (2008).

3.2. Bulk elemental analysis

The particles impacted on each stage of the cascade impactor were analyzed using a proton beam of 2 MeV using an electric current of 10 nA, generated by a 4 MV Van de Graaff electrostatic accelerator installed at PUC-RIO, Brazil, (PIXE technique). Elemental composition of airborne particles collected by the two-stage filter unit were analyzed by a Spectrace-5000 equipped with a Rh-anode X-ray tube that generates a 17.5 W. For the determination of Fe, a high voltage of 35 kV, current of 0.35 mA and acquisition time of 10,000 s was used (EDXRF technique). Other details of EDXRF are presented in Spolnik et al. (2005).

Table 1
Summary of aerosol sampler and measuring techniques.

Aerosol Sampler	Measuring Technique	Year of Oceanographic Cruises			
		2002	2003	2004	2005
six stage cascade impactor	PIXE	X			
two stage "May impactor"	EPMA		X	X	
two stage stack filter unit	EDXRF		X	X	X

Please cite this article in press as: Evangelista, H., et al., Inferring episodic atmospheric iron fluxes in the Western South Atlantic, Atmospheric Environment (2009), doi:10.1016/j.atmosenv.2009.11.018

3.3. Individual particle micro-analysis

Particles collected by the two-stage "May cascade impactor" were submitted to automated EPMA (Ro et al., 1999; Godoi et al., 2004). Electron beam was obtained from a JEOL 733 electron probe micro-analyzer that employed an accelerating high voltage of 10 kV, current of 1.0 nA and measuring time of 20 s. Samples were previously conditioned in liquid nitrogen to reduce destructive effects (mainly the carbon enriched particles) while submitted to high energy electron beams. Quantification by EPMA (including Z-low elements as C, N and O) was made using a Monte Carlo iterative simulation and by the hierarchical cluster analysis performed by an Integrated Data System – IDAS, described in Bondarenko et al. (1996). In EPMA, abundance percentage observed refers to percentage of all particle number counted.

Some distinctive particle types were named according to their major chemical species and concentrations. Since EPMA allows determining the chemical species, at least semi-quantitatively, some individual particles were identified as internally or externally mixed particles. Soil dust abundances were estimated by summing the aluminum and silicon contents in wt% containing trace concentrations of Fe, Ca, K, Ti or Mn (<10% wt). Carbonaceous particles were separated in three different groups of species: biogenic, carbon-rich and organic particles. Particles are identified as organic when the C content is about the same magnitude of O (>70% wt). Mixed organic compounds and soil dust (>10% wt) were found in our samples and were labeled soil dust + organic. The presence of organic coatings over particle was demonstrated earlier for particles suspended in seawater by using an indirect method, but with TW-EPMA we could determine the existence of these layers directly in the X-ray spectra. Fe-containing particles are also encountered and two different types of Fe-containing particles were identified: Fe_2O_3 and Fe metal. Most of Fe metal particles contain 70–80% of Fe with some C and O, due to surface oxidation. In this work, all Fe-containing particles are denoted by "FeO_x". Regarding Fe-containing particles internally mixed with sodium chlorine, we designated as NaCl–FeO_x. Particles were identified as $CaCO_3$ when the stequiometry ratio of Ca, O and C were kept >70% wt. Sodium chloride (sea salt) particles were abundant in coarse and fine modes, which is clearly a fingerprint of the high marine influence on the sampled aerosol. This occurs due to the so-called bubble bursting or sea spray process that transports water drops from bursting white caps into the air, after which crystallization takes place and some salts remain airborne. Therefore, sea salt should be the main constituent in the coarse mode fractions of marine aerosols, except during great episodes of continental dust transport near shore (Fitzgerald, 1991). Since the low-Z EPMA is used for the analysis of a microscopic volume (picogram range in mass for a single particle of micrometer size), the elements at trace levels could not be reliably investigated. Thus, we do not include elements with less than 1.0% of elemental concentration in the procedure of chemical speciation.

3.4. Air mass back-trajectories

At the latitudinal bands where aerosol samples were integrated, the air mass back-trajectories were estimated using NOAA/HYSPLIT Model (Hybrid Single-Particle Lagrangian Integrated – available at http://www.arl.noaa.gov). Ending point for trajectory analyze was at mid-latitude coordinates, 10 m a.s.l.. We used the default meteorological dataset of HYSPLIT, this is, the NCAR/NCEP reanalysis (2.5° lat/long 6 hourly). These trajectories provided information on the retrospective pathway of the air masses before reaching the ship. We run HYSPLIT twice each day (0:00 h and 12:00 h a.m.) for 5 days backwards. An ensemble dispersion product was also used to investigate the uncertainty level attributed to an individual track event, during main peaks of Fe concentration.

4. Results and discussions

4.1. Aerosol composition and microanalyses during 2003, 2004 and 2005 campaigns

Table 2 summaries sampling data of aerosols' collection during 2003, 2004 and 2005 campaigns.

Table 2
Sampling data of 2003, 2004 and 2005 oceanographic campaigns at the Western South Atlantic.

Start of sampling						End of sampling			
Year	ID[d]	Date	Time[c]	Lat (°S)	Long (°W)	Date	Time[c]	Lat (°S)	Long (°W)
2003[a]	1AB	Oct 29th	19:32	22°54′	43°09′	Oct 30th	12:20	25°34′	45°09′
	1CD	Oct 30th	13:15	25°45′	45°19′	Oct 31st	22:05	31°29′	50°21′
	1EF	Nov 9th	02:50	32°13′	52°02′	Nov 10th	19:25	40°01′	53°08′
	1GH	Nov 11th	10:30	42°02′	54°04′	Nov 13th	01:00	48°55′	60°19′
	1IJ	Nov 13th	10:45	50°31′	61°56′	Nov 14th	10:30	55°07′	60°54′
	1LM	Nov 14th	11:20	55°15′	60°52′	Nov 15th	23:25	62°13′	58°18′
2004[b]	2IJ	Feb 15th	14:00	60°59′	55°55′	Feb 16th	18:00	54°56′	56°19′
	2GH	Fev 16th	18:00	54°57′	56°19′	Feb 21st	15:15	42°29′	58°03′
	2EF	Fev 21st	03:15	42°29′	58°03′	Mar 4th	13:20	32°11′	51°52′
	2CD	Mar 4th	13:20	32°11′	51°52′	Mar 6th	06:45	25°53′	45°26′
	2AB	Mar 6th	06:45	25°53′	45°26′	Mar 6th	22:38	23°21′	43°37′
2005[a]	L	Oct 21st	12:00	23.5°00′	44°50′	Oct 22nd	12:00	26.5°00′	44°50′
	M	Oct 22nd	12:00	26.5°00′	44°50′	Oct 23rd	12:00	30.0°00′	51°50′
	N	Oct 23rd	12:00	30.0°00′	51°50′	Oct 24th	12:00	37.5°00′	54°00′
	O	Oct 26th	12:00	37.5°00′	54°00′	Oct 27th	12:00	40.0°00′	56°00′
	P	Oct 27th	12:00	40.0°00′	56°00′	Oct 28th	12:00	44.5°00′	56°00′
	Q	Oct 28th	12:00	44.5°00′	56°50′	Oct 29th	12:00	48.5°00′	56°50′
	R	Oct 29th	12:00	48.5°00′	58°00′	Oct 30th	12:00	50.0°00′	58°00′
	S	Nov 1st	12:00	57.5°00′	59°00′	Nov 2nd	12:00	61.0°00′	59°00′
	T	Nov 4th	12:00	61.0°00′	59°00′	Nov 5th	12:00	62.5°00′	63°00′

[a] Trajectory: from Brazil to Antarctica.
[b] Trajectory: from Antarctica to Brazil.
[c] Time GMT.
[d] ID: Identification of sampling step.

Please cite this article in press as: Evangelista, H., et al., Inferring episodic atmospheric iron fluxes in the Western South Atlantic, Atmospheric Environment (2009), doi:10.1016/j.atmosenv.2009.11.018

Table 3
Atmospheric Fe concentrations for 2003, 2004 and 2005 oceanographic campaigns at the Western South Atlantic. (ID: sampling identification).

Atmospheric Fe concentrations (ng m^{-3})											
Year: 2003				Year: 2004				Year: 2004			
ID	Fine	Coarse	Total	ID	Fine	Coarse	Total	ID	Fine	Coarse	Total
1AB	72.1 ± 9.4	10.4 ± 1.4	82.5 ± 9.5	2IJ	0.31 ± 0.04	0.10 ± 0.01	0.41 ± 0.04	L	4.09 ± 0.53	BDL	4.09 ± 0.53
1CD	19.2 ± 2.5	1.48 ± 0.19	20.7 ± 2.5	2GH	4.28 ± 0.56	0.42 ± 0.06	4.70 ± 0.56	M	0.80 ± 0.10	BDL	0.80 ± 0.10
1EF	20.7 ± 2.7	2.95 ± 0.38	23.7 ± 2.7	2EF	8.59 ± 1.1	1.27 ± 0.17	9.86 ± 1.1	N	38.1 ± 5.0	BDL	38.1 ± 5.0
1GH	4.76 ± 0.62	0.43 ± 0.06	5.19 ± 0.62	2CD	68.9 ± 9.0	9.35 ± 1.2	78.3 ± 9.0	O	1.3 ± 0.17	BDL	1.3 ± 0.17
1IJ	4.32 ± 0.56	0.43 ± 0.06	4.75 ± 0.56	2AB	14.5 ± 1.9	4.62 ± 0.60	19.1 ± 2.0	P	NM	NM	NM
1LM	6.64 ± 0.86	2.95 ± 0.38	9.59 ± 0.94					Q	BDL	BDL	BDL
								R	0.83 ± 0.11	BDL	0.83 ± 0.11
								S	4.09 ± 0.53	1.01 ± 0.13	5.10 ± 0.55
								T	1.66 ± 0.22	0.04 ± 0.01	1.70 ± 0.22

In samples collected in 2003 campaign, total atmospheric Fe showed a decrease towards higher latitudes. Concentrations in the fine mode were 7–12.7 times higher than in coarse mode from latitude ~22°S to ~55°S (an exception was a ratio of 2.3 found near King George Island). In general, total Fe concentrations can be distinguished in three concentration levels: (1) a major peak at ~22–25°S (closer to the largest urban/industrial sites of Brazil) where total Fe concentration reached a value of 82.5 ± 9.5 ng m^{-3}; (2) an intermediate concentration ranging from 20.7 ± 2.69 to 23.7 ± 3.08 ng m^{-3} at ~26–40°S; and (3) a relatively lower concentration level ranging from 4.75 ± 0.62 to 9.59 ± 1.25 ng m^{-3} at ~42–62°S, that geographically corresponds to the Argentine continental shelf and the Drake Passage, Table 3. At latitudes south of 26–30°S, concentrations in the fine mode decreased steadily southwards, while the coarse mode was relatively constant along the latitudinal band 26–62°S.

Concerning the microanalyses by EPMA, the dust imprint in the 6 latitudinal bands was somewhat comparable to the Fe concentration profile; this is, Fe peak at sampling ID "1AB" coincided with a high dust abundance of ~38% (obtained from the sum of dust particles defined by their elemental composition in Table 4) and Fe-rich particles of ~3.5%; at "1CD" we observed particles relative abundance of ~27.2% for NaCl + FeO, ~1% for SiO and ~3 for dust. The presence of FeO–NaCl structures at lower latitudes (25–31°S) indicates the sea salt attachment over terrigenous particles, probably due to the marine spray activity acting along the transport near sea level. At "1 EF" we observed ~20% of AlSi/$NaCO_4$. In contrast, "1 GH" exhibited dust particles with abundance of only ~3%. It also corresponds to the farthest sampling site from the coast line. Although Fe concentrations were relatively low (4.75–9.59 ng m^{-3}) at latitudes associated to the Patagonian semi-desert, the imprint of dust was measurable at that site, including the presence of AlSi–Fe

Table 4
Particle relative abundance obtained by EPMA technique (fine + coarse modes) for the 2003 oceanographic campaign at the Western South Atlantic. (The two highest relative abundances are in bold).

Identification	Particulate type										Total
1AB	**organic**	**dust**	**dust**	**NaCl-organic**	**$NaCO_3$**	**NaCl**	**$NaSO_4$**	**Fe-rich**	**dust**	**$NaCO_3$**	
No. particles	87	75	70	58	42	31	14	14	7	2	400
Abund.(%)	**21.8**	**18.8**	17.5	14.5	10.5	7.75	3.5	3.5	1.75	0.5	100
Major Elements	O, S, Cl	O, Al, Si, Fe	C, O, Na, Al, Si	C, O, Na, Cl	C, O, Na	O, Na, Cl	O, Na, S	C, O, Na, Fe	C, O, Na, Ca, Fe	C, O, Na	
1CD	**NaCl-organic**	**NaCl + FeO**	**NaCl + FeO**	**CuO_x**	**NaCl**	**Na oxides**	**dust**	**Ca/Na-oxide**	**SiO**	**$NaSO_4$**	
No. particles	43	66	10	18	25	79	8	2	3	30	284
Abund.(%)	15.1	**23.2**	3.52	6.34	8.8	**27.8**	2.82	0.7	1.06	10.6	100
Major Elements	C, O, Na, Cl	O, Na, Cl, Fe	C, O, Na, Fe	C, O, Cu	O, Na, Cl	O, Na	O, N, Na, Si, Ca	C, O, Na, Ca	O, Si	O, Na, S	
1EF	**$NaSO_4$**	**$NaSO_4$**	**AlSi/Na_2CO_4**	**NaCl-organic**	**Na_2CO_4**	**AlSi/Na_2CO_4**	**$CaCO_3$-SiO_2**	**$CaCO_3$**	**$MgCO_3$**	**NaCl-organic**	
No. particles	88	27	11	4	43	76	8	62	55	53	427
Abund.(%)	**20.6**	6.32	2.58	0.94	10.1	**17.8**	1.87	14.5	12.9	12.4	100
Major Elements	C, O, Na, S	O, Na, S	C, O, Na, Si, Al	C, N, O, Na, S, Cl	C, O, Na	C, O, Na, Si, Al	C, O, Si, Ca	C, O, Na,	C, O, Mg	C, O, Na, Cl	
1GH	**$NaCO_3$–$NaSO_4$**	**dust**	**$NaCO_3$**	**Cl-rich**	**NaCl-organic**	**$NaCO_3$**	**organic**	**NaCl-aged**	**NaCl-$MgCO_3$**	**oxides**	
No. particles	73	27	202	43	10	98	13	98	213	35	812
Abund.(%)	8.99	3.33	**24.9**	5.3	1.23	12.1	1.6	12.1	**26.2**	4.31	100
Major Elements	C, O, Na, S	C, O, Na, Si	C, O, Na	C, O, Cl	N, O Cl, P	C, O, Na	C, N, O, S	C, O, Na, Cl	C, O, Na, Mg, Cl	C, O, Na, SCl, Ca	
1IJ	**AlSi-organic**	**$NaSO_4$**	**AlSi-organic**	**$NaSO_4$**	**AlSi-Fe-rich**	**AlSi-organic**	**NaCl-organic**	**NaCl**	**dust**	**AlSi-organic**	
No. particles	19	10	41	25	5	38	121	41	17	18	335
Abund.(%)	5.67	2.99	**12.2**	7.46	1.49	11.3	**36.1**	**12.2**	5.07	5.37	100
Major Elements	C, N, O, Al	O, Na, S	C, O, Al	O, Na, S	N, O, Al, Fe	C, O, Al	C, O, Na, Cl	C, Na, Cl	O, Na, Si	C, N, O, Al	
1LM	**dust-organic**	**Cu-rich**	**dust-organic**	**$NaSO_4$**	**Cl–O–C**	**dust-organic**	**NaCl-organic**	**Fe-rich**	**Ca/Na oxide**	**NaCl–$NaCO_3$**	
No. particles	2	1	20	10	42	33	19	6	10	65	208
Abund.(%)	0.96	0.48	9.62	4.81	20.2	**15.9**	9.13	2.88	4.81	**31.3**	100
Major Elements	C, N, Al	C, N, Cu	C, N, O, Al	O, Na,S	C, O, Cl	C,O,Al	C, Na, Cl, O	O, Fe, C	C, O, Na, Ca	C, O, Na, Cl	

Please cite this article in press as: Evangelista, H., et al., Inferring episodic atmospheric iron fluxes in the Western South Atlantic, Atmospheric Environment (2009), doi:10.1016/j.atmosenv.2009.11.018

and dust-organic particles. Observed organic structures were identified in regions of high marine biological activity and probably are associated to surface adsorption of micro-algae fragments or suspended dissolved organic matter.

$CaCO_3$ was detected in total aerosol particles in the latitudinal band ~32–42°S. A potential source-term of it is the presence of coccolithophorid micro-algae, whose shells are composed basically by calcite. $CaCO_3$ in the atmosphere, near the sea surface, could be the result of the mechanical action of winds. Blooms of these organisms have been reported in the same region by Brown and Podesta (1997). The detection of $CaCO_3$ in the atmosphere of that region coincides with reported data of suspended PIC (Particulate Inorganic Carbon or calcite), obtained from MODIS/Terra database for the Southern Ocean (Balch et al., 2005). According to Signorini et al. (2006), peaks of calcite may occur predominantly in the period December to February. Another characteristic that reinforces the marine origin of $CaCO_3$ structures is the simultaneous occurrence of 2 particles types of NaCl-organic structure (relative abundance of ~13%) and $NaSO_4$ (~27%). Coccolithophorid species are mostly very small organisms (<5 μm) that are covered with 'scales' of calcite, called coccoliths. The organisms normally occur in the top 30 m of the water column, including the very surface, which allow them to be detected by ocean color satellite sensors. The 'scales' (aprox. 2 μm) are shed by the live cells during growth and also at the end of a bloom.

Comparing modeled air mass trajectories and Fe concentrations, one can observe that the higher concentrations, corresponding to "1AB", "1CD" and "1 EF" can not be explained by a direct association to a single HYSPLIT air mass back-trajectory that apparently brings to the sampling site a marine influence, due to easterly winds near the coastal region. Nevertheless, a better description of the continental influence over the air mass can be achieved by the use of the ensemble model, also provided by the HYSPLIT, Fig. 1. Air masses associated to "1AB" clearly have migrated across coastal region, where the samplings took place at the nearest position from land (~150 km). Sampling ID "1CD" and "EF" are also marked by terrigenous influence, contrasting to "GH", "IJ" and "LM" that were under the influence of the tip of South America. Differently from 2003, in campaign of 2004 we have not observed a stepwise decrease in Fe concentrations from tropical to sub-polar latitudes, but it was characterized by an abrupt episode of Fe increase associated to a air mass that has previously advected across a considerable land extension of the Patagonian semi-desert. Increases of Fe in fine and coarse aerosol modes occurred at latitudes 25–32°S ("2CD" in Fig. 2). From the HYSPLIT trajectory profiles, it is clear that the Andean orographic affects the westerly winds, that induce a downslop wind structure from the West Patagonia towards the Atlantic coast.

Similarly to the 2003 campaign, higher apportionment of dust particle in the WSA coast in 2004 was detected far away from the Patagonian semi-desert domain. In 2004, terrigenous particles were present in all latitudinal bands ($NaSO_4/CaSO_4$ and MgO–Fe in sampling ID "2AB"; dust, Fe-rich and Si-reach in "2CD"; NaCl-Fe-rich, dust, Si-rich, Fe-rich and $Ca/NaSO_4$ in "2 EF"; dust, $Ca/NaSO_4$, NaCl-dust and NaCl–FeO_x in "2 GH"; $Ca/NaSO_4$ and NaCl–FeO_x in "2IJ"). The higher relative abundance of "dust particles" (21.5%), Fe-rich (6.12%) and Si-rich (10.8%) particles were coincident to the Fe concentration peak at 25–32°S, Table 5.

Measurements of 2005 Campaign were dedicated to Fe, Si and Al content in total aerosol. Fig. 2 also depicts the latitudinal profile of concentrations and back-trajectories relative to the peaks observed

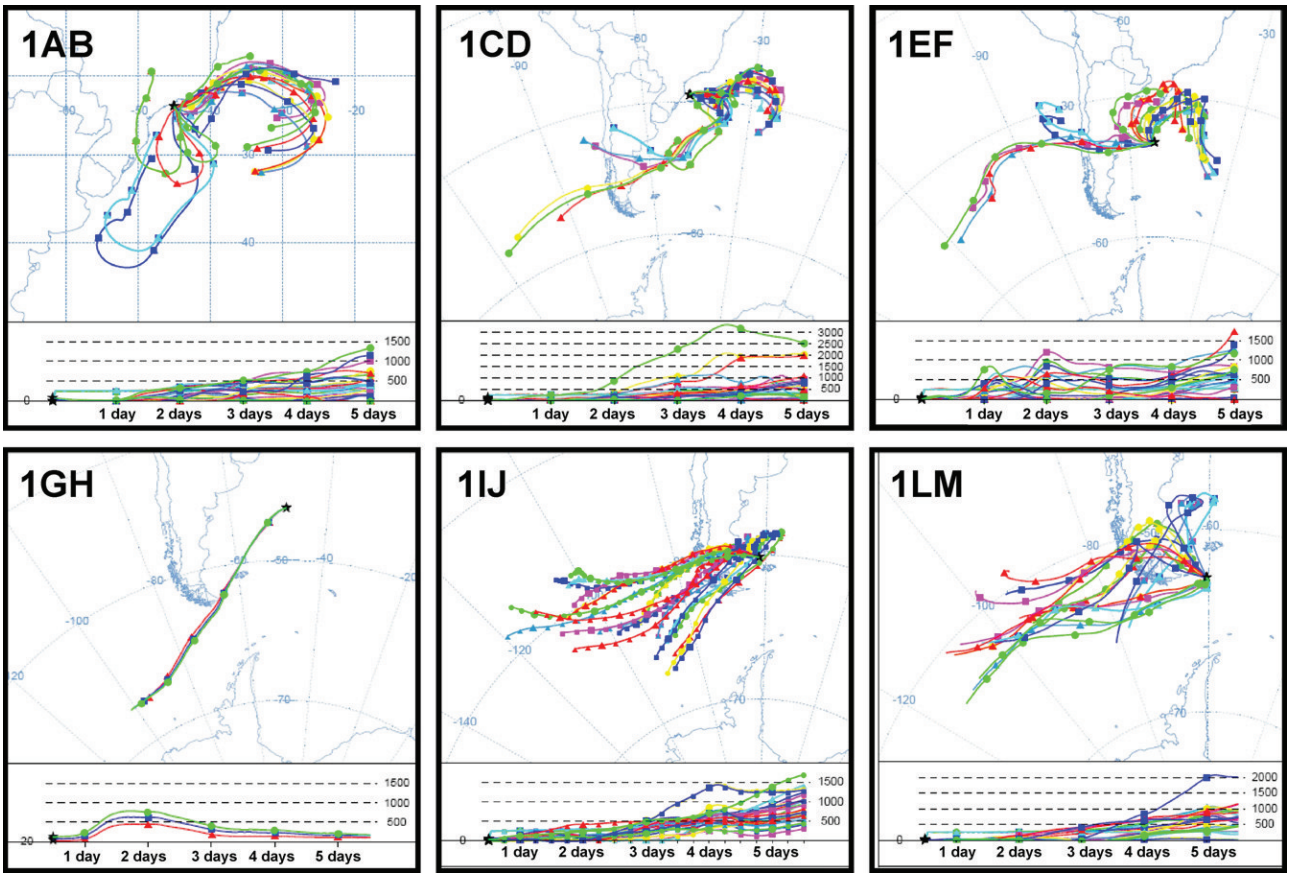

Fig. 1. Five-days air mass back-trajectories associated for the 2004 campaign in the Southwest Atlantic and altitude profile of the trajectories in meters above sea level.

Please cite this article in press as: Evangelista, H., et al., Inferring episodic atmospheric iron fluxes in the Western South Atlantic, Atmospheric Environment (2009), doi:10.1016/j.atmosenv.2009.11.018

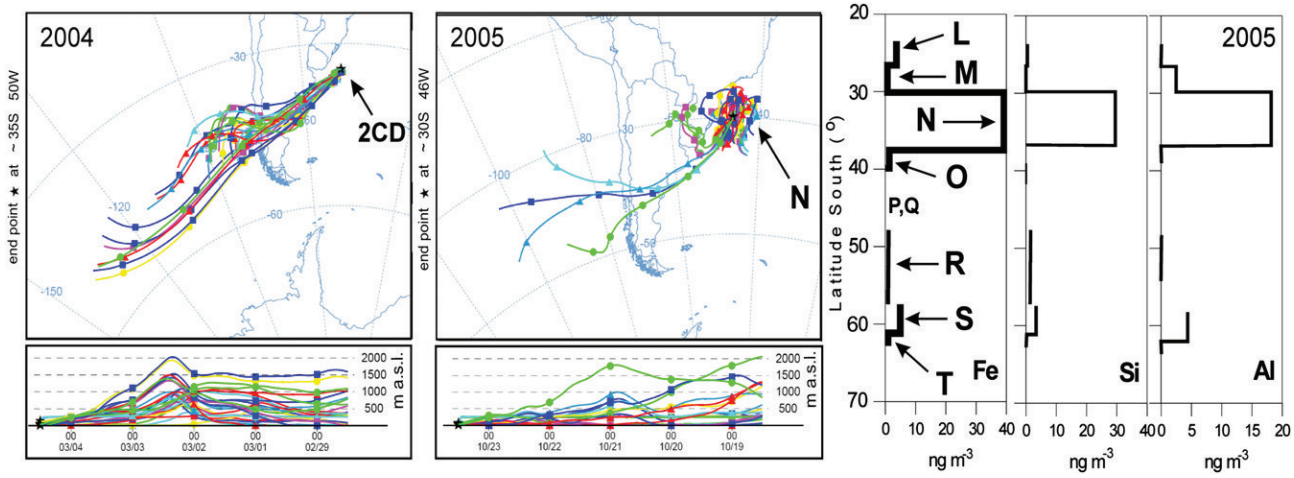

Fig. 2. Five-days air mass back-trajectories associated to the Fe peak during the 2004 (sampling ID "2CD" in Table 1) and 2005 campaign in the Western South Atlantic; (a) illustration of the air mass passage across the Patagonian semi-desert. (Right) profile of total Fe, Si and Al atmospheric concentrations (letters means sampling ID in Table 2).

between ~30°S and 37.5°S (sampling ID "N"). In contrast, the other sampling locations were basically influenced by marine air masses, with restricted migration over the continent. This may explain the relatively low terrigenous concentrations (Fe concentrations were lower than 5 ng m^{-3}) along the campaign.

Considering the air mass trajectories prevailing during 2004 and 2005 cruises (and to a lesser extent 2003), dust/Fe tended to be transported from Patagonia to lower latitudes around 22–40°S. The episodic events observed here constitute a different scenario of models (e.g. Erickson et al., 2003) that assume the dominant westerly winds, blowing from the Patagonian desert to the Argentinean continental shelf at ~40–60°S. If we select the Fe peaks of 2004 ("2CD"), 2005 ("N") and "EF" and "IJ" of 2003 (events associated with advections over Patagonian semi-desert), we see that the atmospheric Fe concentrations tend to increase according to the land extension developed by the air mass, since we found 4.75 ng m^{-3} at ~57°S (event "IJ"), 23 ng m^{-3} at ~38°S (event "EF"), 38 ng m^{-3} at ~33.5°S (event "N") and 78 ng m^{-3} at ~27°S (event "2CD").

4.2. Potential anthropogenic source of atmospheric Fe

Another important point to consider is that the high values of Fe between ~22°S and ~38°S, may include contributions of anthropogenic sources due the proximity to large urban domains like the Cities of Rio de Janeiro and São Paulo located at ~22.5°S and ~23–24°S, respectively, and probably Buenos Aires/Argentina. These metropolises together comprise approximately 40 million people and several industrial sites where Fe are largely emitted. A detailed study of aerosol elemental composition conducted in São Paulo indicated that Fe could be associated either with the fine mode soil dust, related to Ca, Si, Ti and K, or to industry emissions associated with Zn, Mn, Pb, Ni and S (Castanho and Artaxo, 2001). In an important industrial district of Rio de Janeiro (Santa Cruz), aerosols containing Fe were associated with Ca, Mo, Mn, Zn, Cu and Ni (Quiterio et al., 2004). In general, the steel industries are expected to emit Ca, Mn, Cu and Fe. To clarify this, during the 2004 campaign we measured Fe, Pb, Cu, Zn and BC simultaneously. The

Table 5
Particle relative abundance obtained by EPMA technique (fine + coarse modes) for the 2004 oceanographic campaign at the Western South Atlantic. (The two highest relative abundances are in bold).

Identification	Particulate type										Total
2AB	**NaCl-aged**	**NaCl-aged**	**NaCl-aged**	**NaCl**	**$NaSO_4/CaSO_4$**	**$CaSO_4$**	**$MgSO_4$**	**MgO–Fe**	**ClO**	**NaCl-aged**	
No. particles	51	42	38	48	14	5	13	1	2	54	268
Abund.(%)	**19**	15.7	14.2	**17.9**	5.22	1.87	4.85	0.37	0.75	20.2	100
Major Elements	Na, O, Cl	Na, O, Cl	Na, O, Cl	Na, Cl	O, Na, S, Ca	O, S, Ca	O, Mg, S	O, Mg, Fe	C, Cl, Na	C, O, Na, Cl	
2CD	**dust**	**$NaCO_3$**	**Fe-rich**	**Si-rich**	**$CaCO_3$**	**NH_4Cl**	**dust**	**Cl-rich**	**soot**	**S-rich**	
No. particles	116	57	33	58	28	29	73	88	32	25	539
Abund.(%)	**21.5**	10.6	6.12	10.8	5.19	5.38	13.5	**16.3**	5.94	4.64	100
Major Elements	C, O, Si	C, O, Na	C, O, P, Fe	C, O, Si	C, O, Ca	C, N, O, Cl	C, O, Si, Cl	C, O, Cl	C, Cl	C, O, S	
2EF	**NaCl**	**NaCl-aged**	**NaCl-aged**	**NaCl-Fe-rich**	**$Ca/NaSO_4$**	**dust**	**NaCl-organic**	**Si-rich**	**dust**	**Fe-rich**	
No. particles	188	145	106	92	101	28	41	51	31	11	794
Abund.(%)	**23.7**	**18.3**	13.4	11.6	12.7	3.53	5.16	6.42	3.9	1.39	100
Major Elements	Na, Cl	Na, Cl, O	Na, Cl, O	Na, Cl, Fe	O, S, Ca, Na	O, Mg, Al, Si	C, N, O, Na, Cl	O, Si	O, N, Mg, Cu	O, Cl, Fe	
2GH	**NaCl**	**dust**	**$Ca/NaSO_4$**	**NaCl-aged**	**NaCl-aged**	**NaCl-dust**	**NaCl-organic**	**NaCl-aged**	**NaCl–FeO_x**	**$NaCO_3$**	
No. particles	163	92	65	116	223	15	107	102	4	7	894
Abund.(%)	**18.2**	10.3	7.27	13	**25**	1.68	12	11.4	0.45	0.78	100
Major Elements	Na, Cl	O, Si	O, Na, S, Ca	O, Na, Cl	O, Na, Cl	C, N, O, Na, Mg, Cl	C, N, O, Na, Cl	O, Na, Cl	O, Na, Cl, Fe	C, O, Na	
2IJ	**Ca/NaSO4**	**Na/Mg oxide**	**NaCl**	**NaCl-aged**	**Si-rich**	**NaCl-aged**	**Na oxide**	**$NaCO_3$**	**NaCl–FeO_x**	**NaCl-aged**	
No. particles	59	65	103	77	32	81	87	13	4	115	636
Abund.(%)	9.28	10.2	**16.2**	12.1	5.03	12.7	13.7	2.04	0.63	**18.1**	100
Major Elements	O, Na, S, Ca	C, O, Na, Mg	Na, Cl	O, Na, Cl	O, Si	O, Na, Cl	O, Na	C, O, Na	O, Na, Si, Cl, Fe	C, O, Na, Cl	

Please cite this article in press as: Evangelista, H., et al., Inferring episodic atmospheric iron fluxes in the Western South Atlantic, Atmospheric Environment (2009), doi:10.1016/j.atmosenv.2009.11.018

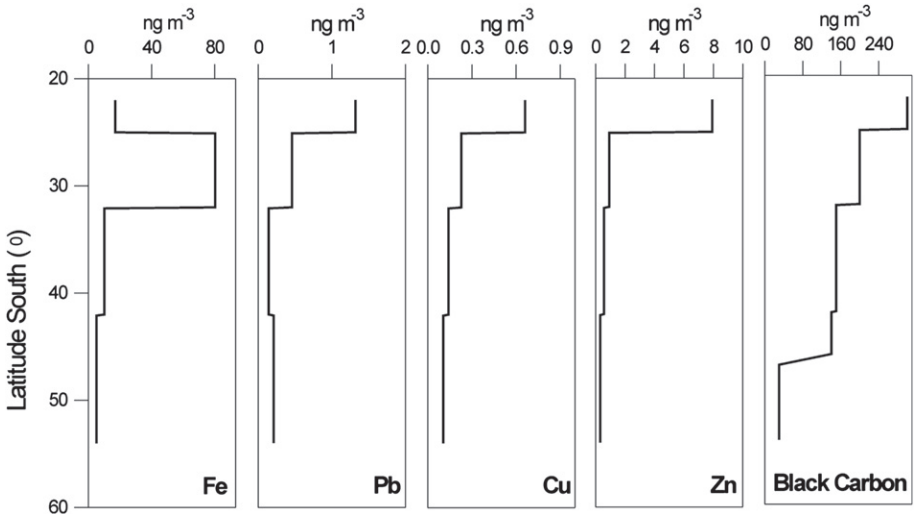

Fig. 3. Latitudinal profile of total Fe, black carbon and tracers of anthropogenic activities (Pb, Cu and Zn), during the 2004 campaign.

latter is carbonaceous particle produced by the incomplete combustion of fossil fuel (also by biomass burning), commonly employed as a tracer of anthropogenic activities, (Evangelista et al., 2007). The on board results indicated that Fe and the set of heavy metals presented different latitudinal profiles; this is, Pb, Cu and Zn exhibited higher concentrations at the boundaries of the urban regions, ~22–25°S, Fig. 3, followed by a sharp decrease southwards, reflecting an atmospheric dilution of the urban/industrial emissions. BC also decreases at about the same latitudes but it remains at relatively high values to finally drop at ~45°S. At the coast of tropical South American at ~32–45°S, Argentine and Uruguay constitute important additional sources of BC (Evangelista et al., 2007; Pereira et al., 2006), while differences exist in their industrial activities. This difference can also be attributed to different aging and removal process among BC, soil dust and particles of urban/industrial sources. For these anthropogenic tracers, the major contribution to the total elemental concentration comprised the fine mode fraction: Cu (89%), Zn (85%) and Pb (62%). By contrast, Fe presented a distinct peak South of 25°S, extending to ~32°S, indicating a decoupling from anthropogenic sources. In order to distinguish the sources of atmospheric Fe, if primarily derived from soil dust or urban emissions, we have compared the ratios BC/Fe obtained on board (cruises of 2003 and 2004) with ratios reported for urban environments (e.g.: the City of São Paulo). We postulated that aerosols containing Fe from Patagonian semi-desert are depleted of BC, while from urban sites they would be internally or externally mixes (Jacobson, 2001) with BC.

BC/Fe data of Castanho and Artaxo (2001) for the summer season (monitored between January and March) and the winter season (July and September) are approximately within the following interval (±1 standard deviation):

$$9.3 \leq \left\{\frac{BC}{Fe}\right\}_{summer} \leq 24 \quad (1a)$$

$$4.8 \leq \left\{\frac{BC}{Fe}\right\}_{winter} \leq 44 \quad (1b)$$

Table 6 summarizes the BC/Fe inventory for the campaigns of 2003 and 2004.

Since the 2003 campaign was conducted in October–November, a more adequate comparison with data of BC/Fe in Table 6 is the interval defined by Equation 1b. In this case, higher Fe concentrations obtained at 22–40°S ("1AB", "1CD"and "1EF") could not, unequivocally, be interpreted as derived from long-range atmospheric transport, although ratios obtained on board were very close to the minimum expected values of the urban environment. In contrast, ratios in latitudes higher than 55°S were far from the interval limits. The 2004 campaign was conducted in February–March and the interval of Equation 1a is adequate. In this case, Fe concentrations corresponding to the peak at ~25°S and 30°S (sampling ID "2CD"), could not be explained by the regional urban sources and corroborate the long-range atmospheric transport as also suggested by the air mass back-trajectory analyses.

Table 6
Ratios of BC/Fe (±1 sd) over sea for 2003 and 2004 oceanographic cruises.

Lat (°S)	2003 Oceanographic cruise			2004 Oceanographic cruise		
	BC (ng m^{-3})	Fe (ng m^{-3})	BC/Fe	BC (ng m^{-3})	Fe (ng m^{-3})	BC/Fe
22°–25°	454 ± 34.5	82.5 ± 10.73	5.51 ± 0.83	500 ± 38.3	19.1 ± 2.48	26.2 ± 4.0
25°–27°	103 ± 9.1	20.7 ± 2.69	4.96 ± 0.78	260 ± 23.3	78.3 ± 10.2	3.3 ± 0.5
27°–30°	103 ± 9.1	20.7 ± 2.69	4.96 ± 0.78	260 ± 23.3	78.3 ± 10.2	3.3 ± 0.5
30°–33°	118 ± 8.5	23.7 ± 3.08	4.99 ± 0.74	236 ± 33.7	–	–
33°–38°	151 ± 6.0	23.7 ± 3.08	6.37 ± 0.87	133 ± 20.5	9.86 ± 1.28	13.5 ± 2.7
38°–40°	62.6 ± 2.1	23.7 ± 3.08	2.64 ± 0.36	108 ± 21.3	9.86 ± 1.28	10.9 ± 2.6
40°–45°	42.7 ± 4.1	5.19 ± 0.67	8.23 ± 1.34	189 ± 15.6	–	–
45°–50°	36.1 ± 3.1	5.19 ± 0.67	6.95 ± 1.08	46.9 ± 7.6	4.7 ± 0.61	10.0 ± 2.1
50°–55°	35.4 ± 2.7	4.75 ± 0.62	7.44 ± 1.12	37.9 ± 4.7	4.7 ± 0.61	8.1 ± 1.4
55°–60°	18.9 ± 2.5	9.59 ± 1.25	1.97 ± 0.37	–	–	–
60°–62°	15.8 ± 2.4	5.59 ± 0.73	2.83 ± 0.57	–	–	–

Please cite this article in press as: Evangelista, H., et al., Inferring episodic atmospheric iron fluxes in the Western South Atlantic, Atmospheric Environment (2009), doi:10.1016/j.atmosenv.2009.11.018

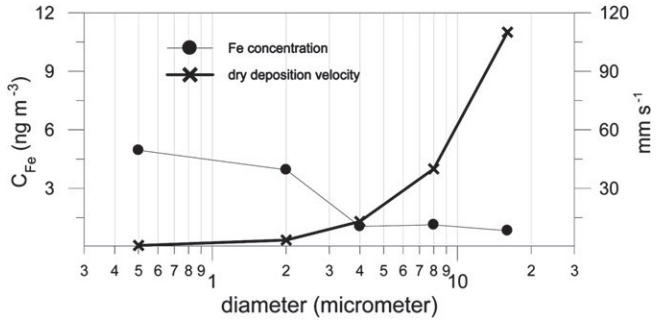

Fig. 4. Measured Fe concentrations (●) and corresponding dry deposition velocities (×) (based on Slinn and Slinn, 1980).

4.3. Fe deposition flux to the sea surface

4.3.1. Dry deposition

Gravimetric deposition velocities of particles (v) onto the ocean generally differ from continental land, due to the distinct surface characteristics and the adhesion of water to the aerosol surface during their transit over the sea, causing them to increase in size. Therefore, the Fe flux derived from dry deposition is better estimated from methods that allow aerosol size distribution. We have estimated the dry flux by two methods: one employing a six-stage cascade impactor during the 2002 campaign, in which one set of filters was used to accumulate a large amount of dust integrated from 25°S to 55°S; a second employing a two-filter holder to collected aerosols in fine and coarse modes. For the first method, the dry deposition flux was calculated by Equation (2):

$$\varphi_{Fe,dry} = \sum_{i=1}^{k} v_i C_{Fe,air,i} \quad (2)$$

where $\varphi_{Fe,dry}$ is the total Fe flux, expressed in nmolFe m^{-2} day^{-1}; v_i is the dry deposition velocities for the i-th diameter of the cascade (according to Slinn and Slinn (1980), considering a mean wind velocity of 5 m s^{-1} measured on board); $C_{Fe,air,i}$ is the i-th Fe concentration; and k is the number of stages used to separate the total sampled aerosol. Fig. 4 shows the results of Fe concentrations and corresponding v_i. For the experiment, the mean Fe deposition flux integrated at 25–55°S was 113 nmolFe m^{-2} day^{-1}. Additionally, we estimated the Fe Mass Median Aerodynamic Diameter (MMAD) to be 0.9 μm.

For the 2003, 2004 and 2005 campaigns, the mean dry deposition was inferred from the two-stage filter unit which associated deposition velocities are 0.001 m s^{-1} for fine mode and 0.02 m s^{-1} for coarse mode, Duce (1991). Based on these considerations, we found 219 nmolFe m^{-2} day^{-1} for 2003 campaign, 127 nmolFe m^{-2} day^{-1} for 2004 and 16 nmolFe m^{-2} day^{-1} for 2005.

4.3.2. Wet deposition

Along the cruise tracks, very few precipitation events have occurred, preventing measurable Fe in rain water ($C_{Fe,rain}$). Nevertheless, it does not mean that regionally it has not occurred. Since the wet deposition estimation requires $C_{Fe,rain}$ values, concentrations in precipitation were alternatively estimated, using the dimensionless below-cloud scavenging ratio, S_r, (Jickells and Spokes, 2001) as follows:

$$\varphi_{Fe,wet} = PC_{Fe,rain}\rho_{rain} \quad (3)$$

where $\varphi_{Fe,wet}$ is in nmolFe m^{-2} day^{-1}, P is the precipitation rate (mm day^{-1}); ρ_{rain} is the rain water density (10^6 g m^{-3}) and $C_{Fe,rain}$ is the Fe concentration in rain (g g^{-1}) which can be expressed as a function of S_r as:

$$C_{Fe,rain} \sim C_{Fe,air}\frac{S_r}{\rho_{air}} \quad (4)$$

where ρ_{air} is the air density (1290 g m^{-3}) at 20 °C and at 1013 hPa. S_r consists in an important part of the uncertainty of the modeled wet deposition component, since S_r is highly dependent on the aerosol size, its hygroscopic characteristics, chemical speciation, atmospheric life history and precipitation intensity (Encinas et al., 2004). Precipitation data employed here (Fig. 5) refers to the period of sampling as described in Section 3. We assumed S_r to be 200, according to Duce (1991), Gao et al. (2003), Sarthou et al. (2003) (for the South Atlantic).

4.3.3. Total deposition

Table 7 presents Fe fluxes in the WSA. Our results clearly identify two concentration levels for total Fe flux with the transition being near latitude 40°S. Two main factors contributed to this difference: (1) during the campaigns, the latitudinal band ~22–40°S received air mass that advected across larger land portions of the Patagonia semi-desert, of Southwest direction, in low altitudes before reaching the sampling sites. Therefore, air masses along there continental migration could be enriched with dust particles

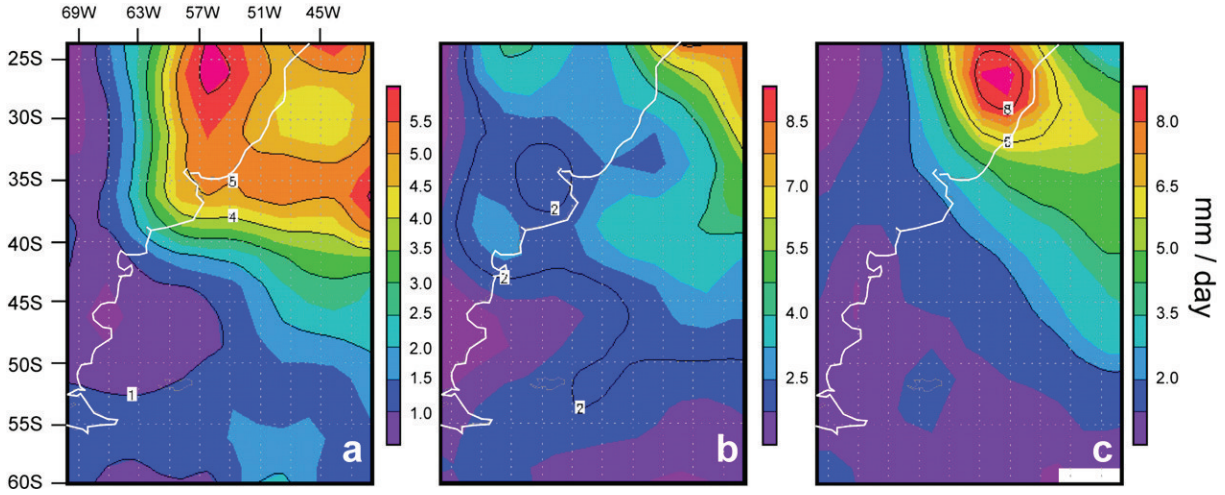

Fig. 5. Precipitation rates (from CDC/NASA) corresponding to the periods of 2003, 2004 and 2005 oceanographic cruises in the Western South Atlantic.

Table 7
Dry and wet Fe fluxes at the Western South Atlantic during the Ary Rongel Oceanographic cruises of 2003, 2004 and 2005.

Year	ID	Rain (mm day^{-1})	Concentration of Fe (ng m^{-3})			Flux (nmolFe m^{-2} day^{-1})		
			Fine	Coarse	Total	Dry	Wet	Total
2003	1AB	5.5 ± 1.1	72.1 ± 9.4	10.4 ± 1.4	82.5 ± 9.5	432 ± 103	1256 ± 300	1688 ± 317
	1CD	4.5 ± 0.9	19.2 ± 2.5	1.48 ± 0.19	20.7 ± 2.5	75.3 ± 18	257 ± 61.0	332 ± 63.9
	1EF	5.3 ± 1.06	20.7 ± 2.7	2.95 ± 0.38	23.7 ± 2.7	123 ± 29.3	347 ± 83	470 ± 87.8
	1GH	0.8 ± 0.16	4.76 ± 0.62	0.43 ± 0.06	5.19 ± 0.62	20.6 ± 4.91	11.5 ± 2.74	32.1 ± 5.63
	1IJ	0.8 ± 0.16	4.32 ± 0.56	0.43 ± 0.06	4.75 ± 0.56	19.9 ± 4.75	10.5 ± 2.50	30.4 ± 5.37
	1LM	1.3 ± 0.26	6.64 ± 0.86	2.95 ± 0.38	9.59 ± 0.94	101 ± 24.1	34.5 ± 8.23	136 ± 25.5
2004	2AB	2.0 ± 0.4	0.31 ± 0.04	0.10 ± 0.01	0.41 ± 0.04	3.56 ± 0.85	2.27 ± 0.54	5.83 ± 1.01
	2CD	1.5 ± 0.3	4.28 ± 0.56	0.42 ± 0.06	4.70 ± 0.56	19.6 ± 4.68	19.5 ± 4.65	39.1 ± 6.60
	2EF	3.0 ± 0.6	8.59 ± 1.1	1.27 ± 0.17	9.86 ± 1.1	52.4 ± 12.5	81.9 ± 19.5	134 ± 23.2
	2GH	5.5 ± 1.1	68.9 ± 9.0	9.35 ± 1.2	78.3 ± 9.0	394 ± 94	1192 ± 284	1586 ± 299
	2IJ	7.5 ± 1.5	14.5 ± 1.9	4.62 ± 0.60	19.1 ± 2.0	165 ± 39.4	397 ± 94.7	562 ± 102
2005	L	4.0 ± 0.8	4.09 ± 0.53	BDL	4.09 ± 0.53	6.31 ± 1.51	45.3 ± 10.8	51.6 ± 10.9
	M	6.0 ± 1.2	0.80 ± 0.10	BDL	0.80 ± 0.10	1.23 ± 0.29	13.3 ± 3.17	14.5 ± 3.19
	N	5.0 ± 1	38.1 ± 5.0	BDL	38.1 ± 5.0	58.8 ± 14.0	527 ± 125	586 ± 126
	O	3.5 ± 0.7	1.3 ± 0.17	BDL	1.3 ± 0.17	2.01 ± 0.48	12.6 ± 3.01	14.6 ± 3.04
	P	1.5 ± 0.3	NM	NM	NM	–	–	–
	Q	1.2 ± 0.24	BDL	BDL	BDL	–	–	–
	R	1.5 ± 0.3	0.83 ± 0.11	BDL	0.83 ± 0.11	1.28 ± 0.31	3.45 ± 0.82	4.73 ± 0.88
	S	1.5 ± 0.3	4.09 ± 0.53	1.01 ± 0.13	5.10 ± 0.55	37.5 ± 8.95	21.2 ± 5.06	58.7 ± 10.3
	T	1.5 ± 0.3	1.66 ± 0.22	0.04 ± 0.01	1.70 ± 0.22	3.80 ± 0.91	7.06 ± 1.68	10.9 ± 1.91

ID: Sampling Identification; BDL : Below Detection Limit; NM : Not Measured.

(including Fe). In contrast, our data of the Patagonian continental shelf were mostly affected by air masses of marine origin and air masses with reduced pathways over the adjacent continental regions. Minor Fe increases observed at the Drake Passage, during 2003 and 2005 campaigns could be attributed to air masses migrating over the tip of South America driven by the dominant zonal wind at that location. The general characteristics of the air mass trajectories observed in our campaigns were somewhat similar of those reported by Baker et al. (2006) in the South Atlantic (~22–47.5°S) in October 2001; (2) despite its favorable aerosol advection, the latitudinal band ~22–40°S is characterized by higher precipitation regime attributed in part by the South Atlantic Convergence Zone (SACZ) and one consequence is a higher wet deposition. From our data, the Patagonian continental shelf was characterized by minor atmospheric Fe concentrations and lower precipitation regime. Considering the relatively short-term period of investigation, our results can be representative of spring-summer conditions, which is coincident to chlorophyll-a peaks in the region (Rivas et al., 2006; Signorini et al., 2006).

5. Summary and conclusions

In this work, we present results of measurements of atmospheric Fe at the coastal region of the WSA. Aerosol samplings were carried out underway, during four oceanographic cruises from the Southeastern Brazil (22°S) to King George Island (62°S), during spring and summer periods from 2002 to 2005. Data was analyzed in conjunction with modeled air mass back-trajectories attempting to identify potential dust/Fe source region. Shipboard measurements exhibited important episodically high atmospheric Fe concentrations during 2004 and 2005 cruises, varying from 38 ng m^{-3} in 2005–80 ng m^{-3} in 2004 at latitudes between 25°S and 38°S, which could not be related with anthropogenic activities. These relatively high values were explained by the back-trajectory analysis of regional air masses that apparently transport Fe enriched aerosols from the Patagonian semi-desert region to lower latitudes in the South Atlantic Ocean. These results suggest that Fe from the Patagonian desert can travel long distances and be deposited over ocean areas very far from the source. Particularly in summer 2004, calcium carbonate was measurable in the atmosphere between 32°S and 42°S, a vicinity region where coccolithophorids have been previously detected by remote sensing techniques. Fe fluxes calculated for the WSA margin varied from 4.73 nmolFe m^{-2} day^{-1} to 1688 nmolFe m^{-2} day^{-1}.

Acknowledgments

The authors thank the Brazilian National Council for Scientific and Technological Development (CNPq)/PROANTAR (Project: 55.0353/2002-0), MMA and SECIRM to have gathered efforts to support this research.

References

Baker, A.R., Jickells, T.D., Witt, M., Linge, K.L., 2006. Trends in the solubility of iron, aluminium, manganese and phosphorus in aerosol collected over the Atlantic Ocean. Mar. Chem. 98, 43–58.

Balch, W.M., Gordon, H.R., Bowler, B.C., Drapeau, D.T., Booth, E.S., 2005. Calcium carbonate measurements in the surface global ocean based on Moderate-Resolution Imaging Spectroradiometer data. J. Geophys. Res-Oceans 110, C07001.

Bondarenko, I., Treiger, B., Van Grieken, R., Van Espen, P., 1996. IDAS: a windows based software package for cluster analysis. Spectrochim. Acta Part B: Atomic Spectrosc 51 (4), 441–456.

Brown, C.W., Podesta, G.P., 1997. Remote sensing of coccolithophore blooms in the western South Atlantic Ocean. Remote Sens. Environ. 60 (1), 83–89.

Bucciarelli, E., Blain, S., Treguer, P., 2001. Iron and manganese in the wake of the Kerguelen Islands (Southern Ocean). Mar. Chem. 73, 21–36.

Cahill, T.A., Eldred, R.A., Barone, J., Ashbaugh, L., 1979. Ambient Aerosol Sampling with Stacked Filter Units. Report Federal Highway Administration FHW-RD-78-178. Davis. Air Quality Group, University of California, pp. 78.

Calzolaia, G., Chiarib, M., Lucarellia, F., Mazzeic, F., Navab, S., Pratic, P., Vallid, G., Vecchid, R., 2008. PIXE and XRF analysis of particulate matter samples: an inter-laboratory comparison. Nucl. Instrum. Methods Phys. Res. B 266, 2401–2404.

Castanho, A.D.A., Artaxo, P., 2001. Wintertime and summertime São Paulo aerosol apportionment study. Atmos. Environ. 35, 4889–4902.

Dias da Cunha, K., Lipsztein, J.L., Fang, C.P., Leite, B.C.V.J., 1998. A cascade impactor to mineral particle analysis. Aerosol Sci. Tech. 29 (2), 126–132.

Duce, R.A., Liss, P.S., Merrill, J.T., Atlas, E.L., Buat-M!enard, P., Hicks, B.B., Miller, J.M., Prospero, J.M., Arimoto, R., Church, T.M., Ellis, W., Galloway, J.N., Hansen, L., Jickels, T.D., Knap, A.H., Reinhardt, K.H., Schneider, B., Soudine, A., Tokos, J.J., Tsunogai, S., Wollast, R., Zhou, M., 1991b. The atmospheric input of trace species to the world ocean. Global Biogeochem. Cycles 5 (3), 193–259.

Duce, R.A., Tindale, N.W., 1991a. Chemistry and biology of iron and other trace metals. Limnol Oceanogr 36, 1715–1726.

Encinas, D., Calzada, I., Casado, H., Andronache, C., 2004. Scavenging ratios in an urban area in the Spanish Basque Country. Aerosol Sci. Tech. 38, 685–691.

Erickson, D.J., Hernandez, J.L., Ginoux, P., Gregg, W.W., McClain, C., Christian, J., 2003. Atmospheric iron delivery and surface ocean biological activity in the Southern Ocean and Patagonian region. Geophys. Res. Lett. 30, 1609.

Evangelista, H., Maldonado, J., Godoi, R.H.M., Pereira, E.B., Koch, D., Tanizaki-Fonseca, K., Van Grieken, R., Sampaio, M., Setzer, A., Alencar, A., Gonçalves, S.C., 2007. Sources and transport of urban and biomass burning aerosol black carbon at the south-west Atlantic coast. J. Atmos. Chem. 56, 225–238.

Fitzgerald, J.W., 1991. Marine aerosols: a review. Atmos. Environ. 25A, 533–545.

Gaiero, D.M., Probst, J.L., Depetris, P.J., Bidart, S.M., Leleyter, L., 2003. Iron and other trace metals in Patagonian riverborne and windborn materials: geochemical control and transport to the southern South Atlantic Ocean. Geochim. Cosmochim. Acta. 67, 3603–3623.

Gao, Y., Fan, S.M., Sarmiento, J.L., 2003. Aeolian iron input to the ocean through precipitation scavenging: A modeling perspective and its implication for natural iron fertilization in the ocean. J. Geophys. Res. 108, D74221.

Gassó, S., Stein, A.F., 2007. Does dust from Patagonia reach the sub-Antarctic Atlantic Ocean? Geophys. Res. Lett. 34, LO1801.

Godoi, R.H.M., Hoornaert, S., Grieken, R.V., 2004. Elemental and single particle aerosol characterization at a mountain background station in Kazakhstan. J. Atmos. Chem. 48, 301–315.

Iriondo, M., 2000. Patagonian dust in Antarctica. Quatern Int. 68, 83–86.

Jacobson, M.Z., 2001. Strong radiative heating due to the mixing state of black carbon in atmospheric aerosols. Nature 409, 695–697. doi:10.1038/35055518.

Jickells, T., Spokes, L.J., 2001. Atmospheric iron inputs to the oceans. In: Turner, D.R., Hunter, K.A. (Eds.), The Biogeochemistry of Iron in Seawater. SCOR-IUPAC, Baltimore, pp. 85–121.

John, W., Hering, S., Reischl, G., Sasaki, G., Goren, S., 1983. Characteristics of Nuplepore filters with large pore size-II. Filtration properties. Atmos. Environ. 17 (2), 373–382.

May, K.R., 1975. An 'ultimate' cascade impactor for aerosol assessment. J. Aerosol Sci. 6, 1–7.

Moore, J.K., Doney, S.C., Glover, D.M., Fung, I.Y., 2002. Iron cycling and nutrient-limitation patterns in surface waters of the World Ocean. Deep-Sea Res. Pt 49, 463–507.

Nuclepore, 1987. Aerosol Multiple Holder Adapters: Assembly and Operating Instructions. Nuclepore Corporation, Pleasanton, pp. 6.

Parker, R.D., Buzzard, G.H., Dzubay, T.G., Bell, J.P., 1977. A two stage respirable aerosol sampler using Nuclepore filters in series. Atmos. Environ. 11, 617–621.

Pereira, E.B., Evangelista, H., Pereira, K.C.D., Cavalcanti, I.F.A., Setzer, A.W., 2006. Apportionment of black carbon in the south Shetland Islands, Antarctic Peninsula. J. Geophys. Res. 111, D03303.

Prospero, J.M., 1981. Arid regions as sources of mineral aerosols in the marine atmosphere. Geologycal Soc. Am. Spec. Pap. 186, 11–26.

Quiterio, S.L., Arbilla, G., Silva, C.R.S., Escaleira, V., 2004. Metals in airborne particulate matter in the industrial district of Santa Cruz, Rio deJaneiro, in an annual period. Atmos. Environ. 38, 321–331.

Rivas, A.L., Dogliotti, A.I., Gagliardini, D.A., 2006. Seasonal variability in satellite-measured surface chlorophyll in the Patagonian shelf. Cont. Shelf. Res. 26, 703–720.

Ro, C.-U., Osán, J., Van Grieken, R., 1999. Determination of Iow-Z elements in individual environmental particles using windowless EPMA. Anal. Chem. 71, 1521.

Sarthou, G., Baker, A.R., Blain, S., Achterberg, E.P., Boye, M., Bowie, A.R., Croot, P.H.J. W., Jicklls, T.D., Worsfold, P.J., 2003. Atmospheric iron deposition and sea-surface dissolved iron concentrations in Eastern Atlantic Ocean. Deep-Sea Res. Pt 50, 1339–1352.

Signorini, S.R., Garcia, V.M.T., Piola, A.R., Garcia, C.A.E., Mata, M.M., McClain, C.R., 2006. Seasonnal and interannual variabilility of calcite in the vicinity of the Patagonian shelf break (38°S–52°S). Geophys. Res. Lett. 33, Li6610.

Slinn, S.A., Slinn, W.G.N., 1980. Predictions for particle deposition on natural waters. Atmos. Environ. 15, 123–129.

Spolnik, Z., Belikov, K., Van Meel, K., Adriaenssens, K., De Roeck, F., Van Grieken, R., 2005. Appl. Spectrosc. 59, 1465–1469.

Please cite this article in press as: Evangelista, H., et al., Inferring episodic atmospheric iron fluxes in the Western South Atlantic, Atmospheric Environment (2009), doi:10.1016/j.atmosenv.2009.11.018